

## ANALYSIS OF CRACK RESISTANCE AND QUALITY OF THIN COATINGS BY ACOUSTIC EMISSION

S.A. Nikulin, V.G. Khanzhin, A.B. Rozhnov, A.V. Babukin, V.A. Belov

119049, Moscow, Russia, Leninsky prospekt, 4,  
E-mails: [nikulin@misis.ru](mailto:nikulin@misis.ru), [khanzhin@nm.ru](mailto:khanzhin@nm.ru), [aeforscc@yahoo.com](mailto:aeforscc@yahoo.com),  
[Alexander\\_17@newmail.ru](mailto:Alexander_17@newmail.ru), [dalv82@nm.ru](mailto:dalv82@nm.ru)

### ABSTRACT

*The Acoustic Emission (AE) method was employed to study the processes of surface crack initiation and evolution in surface protective coatings (Cr coats on superconductors, oxide films on zirconium cladding tubes, thickness up to 8  $\mu\text{m}$ ). Fracture mechanism and kinetics of electrolytic chrome coatings on multifilamentary superconducting wire have been investigated. The objective in this work is to assess the structure and the strength of 3 types of chrome coatings, different in view of their production technologies. AE-diagrams and synchronized with them by the time the diagrams of wire specimens deformation are presented. AE measurements allowed extracting the deformation of the beginning of active chrome destruction at tension. The AE method was applied to investigate the crack resistance of oxide films on zirconium cladding tubes. Stresses were determined that effect primary cracks and the kinetics of their evolution in oxide films having various thickness was studied. The AE parameters were identified that characterize the oxide resistance to cracking which allows the forecast of the failure onset for an oxide film on items during tests and operation. The dependence of a log of total amplitude AE on thickness of a protective oxide film characterizing the oxide coat crack resistance is presented.*

**Keywords:** Acoustic emission, Coats, Layers, Surface, Superconductor, Zirconium tube

### 1. Introduction

Electrical losses of superconducting cable, being used to create magnetic systems of alternative and pulse field, are decreased when high resistive insulating coatings are applied [1]. The coating should have satisfactory electrophysical properties, good heat conductivity, sufficient mechanical strength and plasticity. Highly resistive electrolytically produced chrome coatings on stabilized Nb<sub>3</sub>Sn superconductors 0.81 mm dia, designed for creation of the ITER magnetic system [2], were studied in this work. The objective in this work is to assess the structure and the strength of 3 types of chrome coatings, different in view of their production technologies, for choice of the best coating quality. Strength characteristics of chrome electrolytical precipitates were determined using the measurements of acoustic emission (AE) at the wire specimen tension.

Zirconium cladding tubes of the nuclear reactors are subjected to various types of corrosion because of interaction with water and fuel fission products during operation. Made by oxidation

at the stage of tube manufacturing oxide films can serve as protective coats against corrosion. However, influence of various mechanical operational loading can lead to oxide film cracking. It leads to acceleration of cladding corrosion and reduction of an operational resource of fuel rods. Therefore it is important to estimate the crack resistance of oxide films (coats) during mechanical loading. The majority results obtained, concerning the oxide films on zirconium, first of all, describe the microstructural aspects and growth kinetics. Because of difficulties of thin film research, the majority of experiments are carried out using specimens with film thickness more than 10 microns.

## 2. Experimental

### 2.1 Investigation of High-Resistive Chrome Coatings Cracking

Highly resistive chrome coating were applied electrolytically on multifilamentary stabilized Nb<sub>3</sub>Sn-based superconductors of 0.81 mm dia with 7225 niobium filaments in Cu-Sn bronze matrix (60% Cu volume fraction). Non-copper current density of this conductor was 590 A/mm<sup>2</sup> at 12 T, and hysteresis losses were 160 MJ/cm<sup>3</sup> (non-copper) at ±3 T. The electrolytical chrome coatings of 3 types - hard Cr (Vickers hardness HV = 700-800), milk Cr (HV = 400-500) and black Cr (HV = 300-400) - were prepared by changing of the electrical current density, the composition and the temperature of electrolyte, and the duration of the process. The thickness of coatings of all the 3 types were made up 1, 3 and 8 μm.

Wire specimens 0.81 mm in dia and with working part length 50 mm with and without chrome coating were tested for tension on a universal break-machine of "Instron"-type with the velocity 1.2 mm/min at temperature 20 °C.

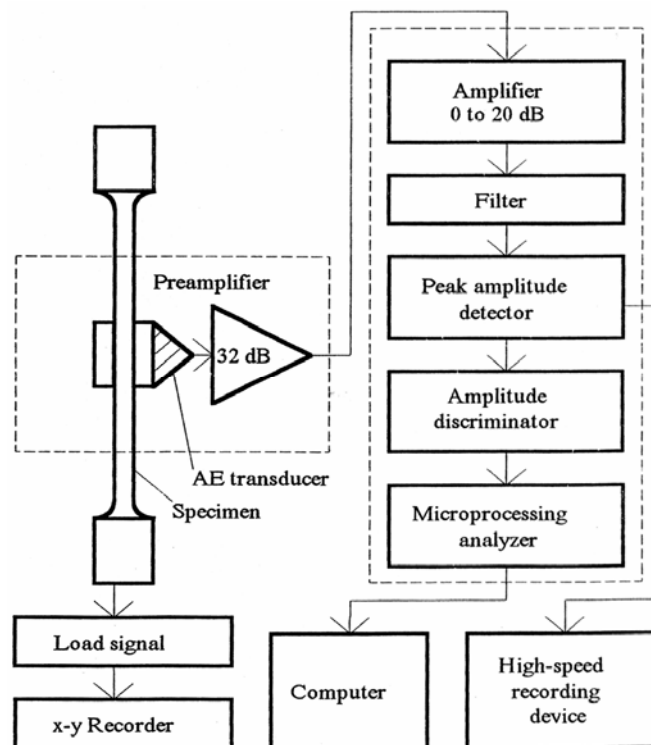


Fig. 1: Block diagram of AE measurement instrumentation used in the experiment.

Acoustic emission was measured with the apparatus, especially designed for testing small-size specimens of superconducting composite materials for tension, bending and twisting. A schematic model of the instrument is shown in fig. 1. Detecting of acoustic emission (AE) at the

destruction of chrome was performed by an acoustic detector from free working part of specimen.

AE pulses were registered lineary (by level  $\pm 3$  dB) within the frequency range of 0.01 to 10 MHz and dynamic range of amplitudes 72 dB. The level of own noises, brought into the inlet of electron apparatus,  $U_n = 10^{-5}$  V. The detected signal was recorded and processed with a specially designed microprocessor analyzer of AE signals (MAS) [3]. The MAS carries out the collection, transformation, preliminary processing, and output to a self-printer in digital and analog forms of the results of the destruction process kinetics quantitative analysis.

Relative sizes of microdestruction centers were evaluated by the level of peak amplitudes of AE pulses  $U_p$ . The relation between peak AE amplitudes with material plasticity is determined by the velocity of elastic energy release at the crack formation [4]. For a brittle crack, breaking-up with the velocity close to the velocity of sound, the amplitude of acoustic pulse is proportional to peak power of elastic energy scattering. As a source of elastic waves, ductile cracks are characterized by low power of elastic energy being released, and therefore, low level of AE amplitudes [4], [5].

The analyzer program allowed automated measurement at the acoustic noise level  $U_n$  at an area where the Kaiser effect applies [6], and the decibel digitization of all amplitudes of acoustic signals relative to the noise level  $V_p = 20 \times \lg(U_p/U_n)$  in real time.

Morphology of chrome surface and microstructure were studied at a scanning electron microscope YEM-100 CXZ at magnifications x300-6000.

## **2.2 Analysis of cracking resistance of oxide films on zirconium cladding tubes**

In view of small thickness of protective zirconium films, their mechanical properties are not studied well. For studying behavior of a film upon mechanical loading, application of high-sensitivity methods is necessary; one of which is measurement of acoustic emission (AE). We have showed the opportunity of the deformation and fracture processes analysis of thin layers and coatings by AE-measurements earlier [7, 8].

In the present work the technique of crack resistance estimation of oxide coats on cladding tubes is presented. The technique based on AE-measurement of cracks developing upon static loading of tubular specimens in a special mandrel. Static loading of specimens by internal pressure is lead to an opening existing in oxide film cracks or led to formation of new cracks. These processes were accompanied by AE -impulses registered by the piezoelectric transducer, fixed directly on the specimen. Further, by means of the special equipment [8] signals were transferred in a personal computer for the subsequent processing and allocation of AE informative parameters.

## **3. Results and discussion**

### **3.1 Chrome Coatings**

Fig. 2 presents the microphotos of chrome coating surface after deformation. Parameters of the chrome grain structure are given in table I. The most imperfect are one-micron coatings hard Cr. The density of defects in one-micron coatings milk Cr is lower.

As known, chrome cracks can be formed at the stage of electrolytical precipitation. Therefore, cracks are observed on the surface of not only deformed, but also non-deformed coatings of chrome at thickness 3 and 8  $\mu\text{m}$ . The greatest density of cracks is observed on black Cr coatings both before and after deformation. However, if coatings black Cr has all the cracks lateral with a small cracking with bank opening  $\delta_{\text{max}} = 0.8-1.0 \mu\text{m}$ , then the cracks of coatings hard Cr create already before deformation a grid of longitudinal and lateral cracks with  $\delta_{\text{max}} = 5-15 \mu\text{m}$ .

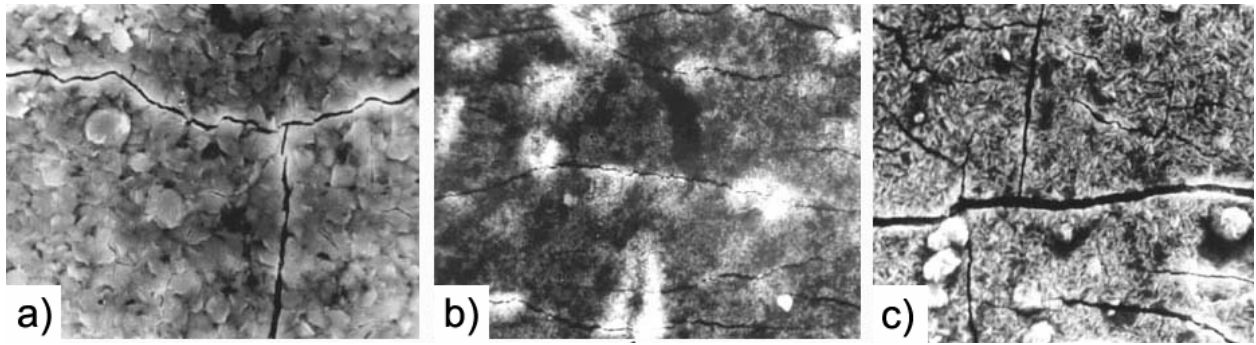


Fig. 2: Structure of Cr-coating after deformation: (a) –milk Cr;  
(b)-black Cr, (c) – hard Cr, x1000.

AE measurements allowed extracting the deformation of the beginning of active chrome destruction at tension  $\varepsilon_1$ . Kinetics of damage accumulation was studied by integral functions of number of AE pulses specimen deformation:  $\sum N(\varepsilon)$ . Fig. 3 shows typical AE-diagrams and synchronized with them by the time works the diagrams of wire specimens deformation. There the kinetic functions  $\sum N(\varepsilon)$  and types of histograms of AE pulses amplitude distributions are also presented. Fig. 4 shows the relationship between the deformations  $\varepsilon_1$  and the coating thickness for all types coatings.

Table 1: Structure characteristics of chrome coatings.

Type of coating	Thickness, $\mu\text{m}$	Shapes and sizes of grains	Texture
Hard chrome	1	Round, (2-3) $\mu\text{m}$	no
	3	Extended, (5-15) $\mu\text{m}$ (1-2) $\mu\text{m}$ Needle, (1,5-2,5) $\mu\text{m} \times$ 0,2 $\mu\text{m} \times$ 0,4 $\mu\text{m}$	Along the specimen axis  no
	8	Plate, 1,5 $\mu\text{m} \times$ (4-5) $\mu\text{m}$	Along the specimen axis
Milk chrome	1	Round, (0,2-0,5) $\mu\text{m}$	no
	3	Plate, (1,5-2) $\mu\text{m} \times$ (2,5 –3) $\mu\text{m}$	no
	8	Extended, (1,8-2,5) $\mu\text{m} \times$ (3-7) $\mu\text{m}$	no
Black chrome	1	Round, (0,1-0,2) $\mu\text{m}$	no
	3	Round, (0,3-0,5) $\mu\text{m}$	no
	8	Round, (0,4-0,8) $\mu\text{m}$	no

The coating hard Cr is the least stable to tension strain ( $\varepsilon_1 = 0.50-0,65\%$ ) at all the thickness. If for coatings hard Cr the decrease of  $\varepsilon_1$  with the thickness is not statistically important then for coatings milk and black Cr the decrease of  $\varepsilon_1$  with the coating thickness growth is considerable. Kinetic curves of damages accumulation  $\Sigma N(\varepsilon)$  at the deformation of specimens with one-micron coatings of all types are of the form of parabola and have narrow amplitude AE distributions (fig. 3).

The parabolic function  $\Sigma N(\varepsilon)$  remains the same at  $h = 3 \mu\text{m}$  for coatings milk and black Cr. For coatings hard Cr ( $h = 3 \mu\text{m}$ ) after deformation  $\varepsilon_2 = 3.5-4.6\%$  the AE intensity is increased. Exponential section appears on functions  $\Sigma N(\varepsilon)$ , amplitude spectrum AE expands (fig. 3). For coatings milk ( $\varepsilon_2 = 4-5\%$ ) and black ( $\varepsilon_2 = 5-7\%$ ) Cr the short exponential section of functions  $\Sigma N(\varepsilon)$  was observed only at coatings thickness  $h = 8 \mu\text{m}$ .

The resistive coatings produced by the hard Cr technology have the least strength. At thickness  $h = 1 \mu\text{m}$  the coating destruction takes place with the formation of short cracks (with average length  $L = 20 \mu\text{m}$ ) on the defects of coating surface (fig. 2). At deformation of thin chrome layers the amount of "weak" places (places of cracks origination) due to initiation of destruction centers, is reducing continuously. Small chrome thickness and defects retard the development of new cracks being formed. Therefore, integral functions  $\Sigma N(\varepsilon)$  in this case are parabolas (fig. 3). Coatings hard Cr have at thickness  $h = 1 \mu\text{m}$  the highest friability ( $V_p = 45 \text{ dB}$ ), compared to a relatively plastic coating milk Cr ( $V_p = 25 \text{ dB}$ ) and ductile black Cr ( $V_p = 18-20 \text{ dB}$ ).

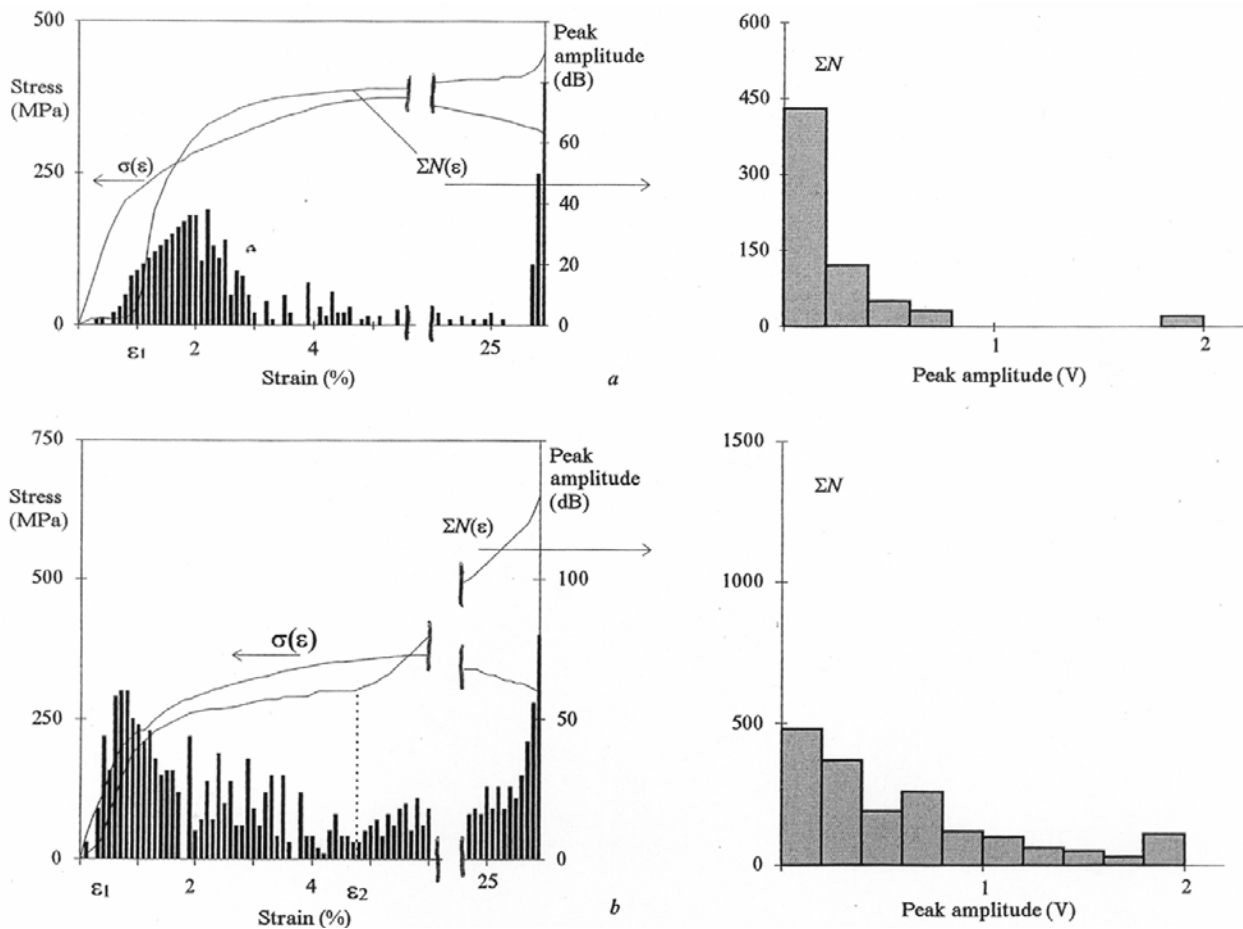


Fig. 3: Typical AE diagrams, stress-strain curves, kinetic functions  $\Sigma N(\varepsilon)$  and types of histograms of AE peak amplitude distributions:  
 (a) – milk Cr coating; (b) – hard Cr,  $h=3\mu\text{m}$ .

Change in coating thickness by changing the structure and changes the density of cracks induced at electrolytical precipitation. The increase of porosity of coatings black Cr at the comparable with coatings milk Cr density of induced cracks reduces  $\varepsilon_1$  from 1.2% at  $h = 1 \mu\text{m}$  to 0.8% at  $h = 3 \mu\text{m}$  (fig. 4). If brittle cracks in coatings hard Cr have great openings of banks and comparatively straight paths, then the main-line cracks in coatings black Cr consist of short ( $L = 50 \mu\text{m}$ ) tortuous sections, each of which was apparently formed in the plastic zone of neighboring ones.

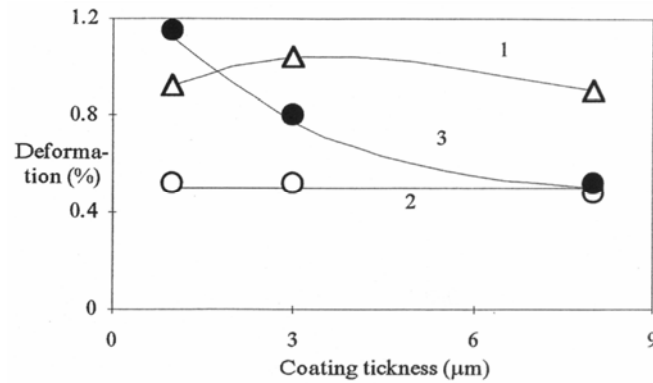


Fig. 4: Relationship of deformation of the beginning of coating destruction to coating thickness: (1) - milk Cr; (2) - black Cr; (3) - hard Cr.

The development of destruction at chrome thickness  $h = 8 \mu\text{m}$  goes with the expansion of electrolytical cracks, therefore by values  $\varepsilon_1$  the hard and black coatings are not greatly different (fig. 4). The increase of AE intensity at the exponential stage of the chrome destruction kinetics is not accompanied by a sharp increase in the surface cracks density. This made it possible to presume that the process of formation internal microcracks determines the secondary chrome cracking being released by AE.

### 3.2 Zirconium films

By means of the developed technique tests have been carried out of cladding tubes specimens made of alloy E110 (Zr-1%Nb) with oxide coats of different thickness - from 1,7 microns up to 8,3 microns. Static deformation of specimens with coats was accompanied by AE with amplitudes from 100 up to 1000 in standard units from formation and opening of cracks. Greater AE intensity and amplitude (Fig. 5) have characterized specimens with thicker oxide coats.

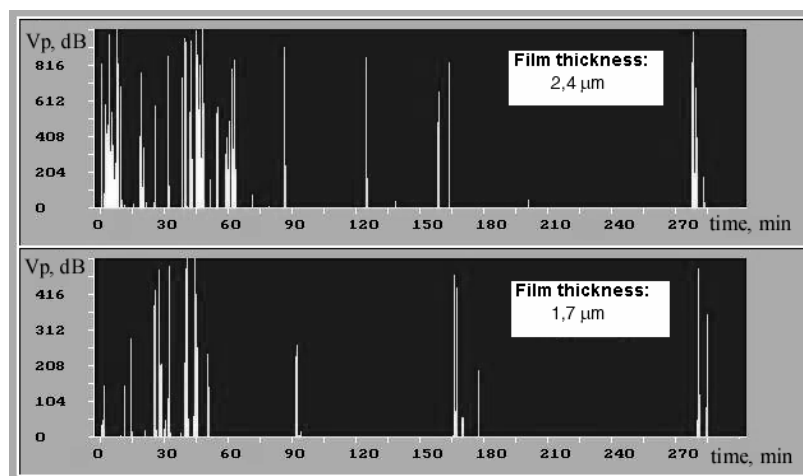


Fig. 5: Typical AE-diagrams upon tube testing with different thickness of oxide.

SEM investigation of specimens after tests have been shown, that intensive AE is determined by the type and the sizes of cracks in oxide film. Tests of specimens with different thickness of oxide films have revealed different morphology, size and an arrangement of cracks in oxide layer (Fig. 6). In this analysis characteristic types of defects are allocated for film surfaces: internal individual cracks on metal/oxide interface in thin films (fig. 6a), small groups of through-film transverse cracks for average thickness layers (fig. 6b), grids of cracks in "thick" oxide films (fig. 6c).

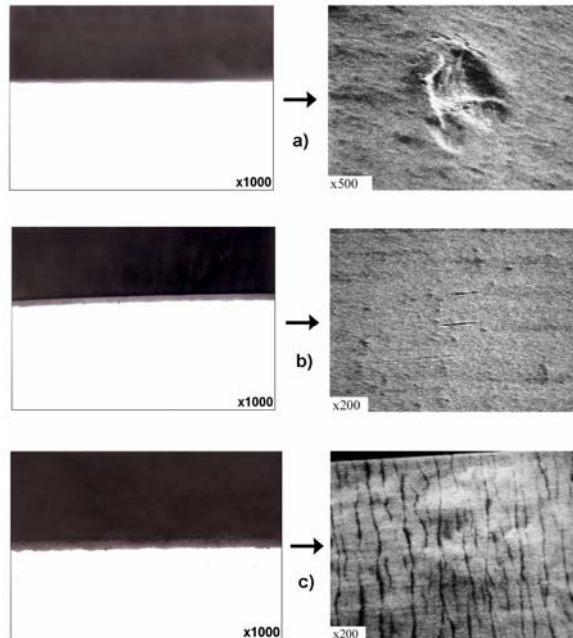


Fig. 6: Defects in oxide films with different thickness after tube loading (a-1,7  $\mu\text{m}$ , b- 4  $\mu\text{m}$ , c-8,3  $\mu\text{m}$ ).

Formation of each type defects in films is accompanied by characteristic AE, allocated at processing signals. Sizes of formed defects are estimated by amplitude of AE impulses (the more impulse – the larger crack). AE-measurements have shown, that if increase the thickness of oxide film more than 1,7- 2,0 microns, AE intensity considerably increase, that testifies to falling crack resistance because the deficiency increase (fig. 7).

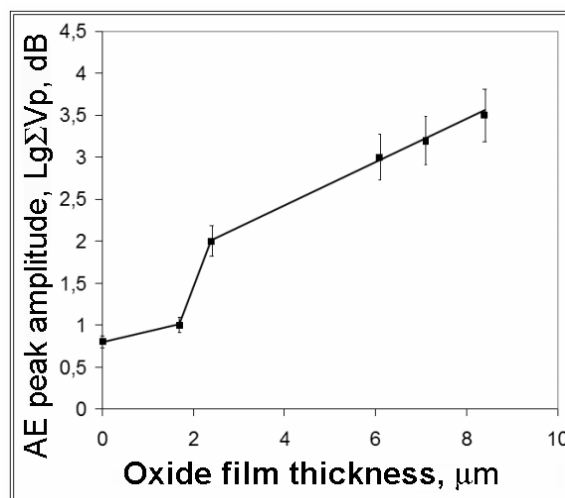


Fig. 7: Dependence of AE amplitude ( $\text{Lg}\Sigma V_p$ ) on oxide film thickness (h).

#### 4. Conclusions

Fracture mechanism and kinetics of electrolytic chrome coatings on multifilamentary Nb<sub>3</sub>Sn-based superconducting wire have been investigated with AE method. AE measurements allowed extracting the deformation of the beginning of active coating destruction at tension. Milk Cr coatings are shown to have the greatest strength at any coating thickness, the same is for black Cr but at thickness of 1 to 3 μm. In these coatings the cracks formation is going by the ductile mechanism. Hard Cr coating have the least strength at any thickness.

Constructed on AE-measurements calibration dependencies "peak amplitude of AE - film thickness" allow to estimate directly oxide film deficiency, tie strength on metal/oxide interface and a plasticity margin of films on a surface of cladding tubes. It makes possible definition of oxide film thickness at that begins it peeling or cracking at the given stress, or, at the given thickness of a film - to define stresses and deformations causing cracking. This allows predicting oxide film fracture during testing or operation of cladding tubes in nuclear reactors.

#### 5. References

- [1] Bussier D. F.: Superconductors for electricity transfer lines. In book: "Metallurgy of superconducting materials" (In Russian), Moscow, Metallurgy, 1983, pp. 192-238.
- [2] Nikulin A. D., Shikov A. K., Silaev A. A., IEEE Transaction on Magnetics, Vol. 30, No. 4, 1994, 2316-2319.
- [3] Khanzhin V. G., Tumanov A. V., Nikulin S. A.: (In Russian), Prib. Texh. Ehks., No. 1, 1991, 241.
- [4] Khanzhin V. G., Shtremel M. A., Nikulin S. A.: (In Russian), Defektoskopiya, No. 4, 1990, 35-40.
- [5] Nikulin S. A., Shtremel M. A., Khanzhin V. G.: Influence of Hydrides on Ductile fracture in the Zr-2,5%Nb alloy, Nuclear Science and Engineering, Vol. 115, 1993, 193-204.
- [6] Karser J., PhD Thesis, Hochshull, Muncher, Germany (1950), see also Arch. Eisenuttenwes, 24, 1953, 43.
- [7] Nikulin S.A., Khanzhin V.G., Rozhnov A.B. Peregud M.M.: Acoustic Emission Monitoring of Zr alloy Deformation and Fracture. Proceedings (Abstracts) of the 13th International Symposium on Zirconium in the Nuclear Industry, Annecy, France, 2001, 58-59.
- [8] Nikulin S.A., Shtremel M.A., Khanzhin V.G., et al.: The analysis of fracture scale and material quality monitoring with the help of acoustic emission measurements, in: Acoustic Emission: Standards and Technology Update, ASTM STP 1353, 1998, 125-140.